CrossMark

Will the western Pacific subtropical high constantly intensify in the future?

Yanyan Huang[1] · Xiaofan Li[1] · Huijun Wang[2]

Abstract The western Pacific subtropical high (WPSH) features lower-level southerlies or southwesterlies at its western and southern edges that transport amount of water vapor into East Asia, and it exerts a large influence on the East Asian summer climate. This paper evaluates the historical (1950–2005) spatial distribution and variability in the summer WPSH at 850 hPa using 28 general circulation models from the Coupled Model Intercomparison Project Phase 5 (CMIP5) relative to the NCEP–NCAR reanalysis data. To avoid the artificial influence caused by global warming, this study primarily investigates the 850-hPa eddy geopotential height and the horizontal winds. The results show that most of the CMIP5 models reliably reproduce the geographical distribution and spatial variability in the WPSH. Four models (bcc-csm1-1, CESM1–CAM5, GFDL–ESM2G and inmcm4) generally perform well in simulating the eastward-recessed interdecadal variation in the WPSH during 1979–2005 relative to 1950–1978, with a significant cyclone anomaly appearing over the western Pacific and a decreasing trend in the WPSH index. Based on these four models, a multi-model ensemble projects a weaker WPSH during 2026–2070 relative to 2010–2025 and 2071–2100 under the representative concentration pathway 8.5 scenario.

1 Introduction

The western Pacific subtropical high (WPSH) is a large-scale anticyclonic circulation located over the subtropical Pacific throughout the year and reaches its peaking phase in summer. The WPSH has large influences on the East Asian summer climate (Zhu et al. 2000). Its low-level western edge features southerlies and southwesterlies that deliver a large quantity of water vapor into East Asia. The intensity, shape and location of the WPSH consequently dominate the large-scale quasi-stationary frontal zones (Huang and Yu 1962; Tao and Xu 1962; Tao and Chen 1987; Chang et al. 2000) and the temperature in East Asia (Hu 1997; Chen et al. 2001). Additionally, the influence of the WPSH can also be examined based on its interactions with other Asian circulations. The WPSH has been identified as a dominant component of the East Asian summer monsoon (EASM). The seasonal northward shifts of the WPSH are closely associated with the onset and withdrawal of the EASM (Tao 1963; Lau and Li 1984; Tao and Chen 1987; Huang and Wu 1989; Ding 1994; Zhu et al. 2010; Wang and Chen 2012; Huang et al. 2013a, b). The seasonal northward advance of the WPSH also corresponds to the seasonal movements of the South Asian high (Tao and Zhu 1964; Zhang and Wu 2001), the westerly jet (Li et al. 2004; Zhao et al. 2005; Kuang and Zhang 2006) and the East Asian blocking situation (Liao and Zhao 1990; Zhang and Tao 2003).

Many factors have been suggested to explain the formation and maintenance of the WPSH. The impact of the Tibet plateau, which acts as a robust heating source to the

✉ Yanyan Huang
yanyanhuang@zju.edu.cn

[1] School of Earth Science, Zhejiang University, Hangzhou 310027, China

[2] Nansen-Zhu International Research Centre, Institute of Atmospheric Physics, Chinese Academy of Sciences, Beijing 100029, China

atmosphere in the summer, was proposed first (Ye and Gao 1979; Ye and Wu 1998). Additionally, anomalies in the sea surface temperature (SST), which can affect the atmospheric convections and trigger dynamic waves, also play an important role (Huang and Sun 1994; Lu and Dong 2001; Wang et al. 2013a). Moreover, the monsoon diabatic heating (Ting 1994; Hoskins 1996; Rodwell and Hoskins 2001), the land-sea heating contrast (Wu and Liu 2003; Miyasaka and Nakamura 2005) and the air–sea interaction (Seager et al. 2003) have also been proposed.

The WPSH has been shown to exhibit multi-scale temporal variations. Its interannual variability (e.g., Huang and Yu 1962; Tao and Xu 1962; Sui et al. 2007; He et al. 2012) and its relationship with tropical cyclone activity over the western North Pacific (Chia and Ropelewski 2002; Zhou and Cui 2008) have been studied for decades. To quantify its interannual variability, the atmospheric variables at 500 hPa have been most commonly used to define the WPSH indices, especially for geopotential height (e.g., Huang 1963; Tao and Chen 1987; Sun and Ying 1999), as well as relative vorticity (Yang and Sun 2003). Recent studies have also used the climate variables at 850 hPa, such as the geopotential height (Lu 2002; Wang et al. 2013a), the horizontal winds (Wang et al. 2001; Huang et al. 2010) and the relative vorticity (Lu et al. 2008).

Based on the investigation of the interdecadal position change in the 588 dagpm contour line at 500 hPa, previous studies have noted that the WPSH has extended westward since the 1970s (Nitta and Hu 1996; Hu 1997; Gong and Ho 2002). Its westward extension has been suggested to contribute to the increased rainfall over the middle and lower reaches of the Yangtze River valley and decreased rainfall over North China since the late 1970s (Gong and Ho 2002), as well as decadal variations of temperature in East Asia (Hu 1997) and typhoon tracks over the western North Pacific (Gong and He 2002; Ho et al. 2004). The Indian Ocean–western Pacific warming has been proposed to be responsible for this westward-extended WPSH (Zhou et al. 2009). However, Yang and Sun (2003), Lu et al. (2008) and Huang and Li (2015) argue that the direct use of the geopotential height field to examine the interdecadal variation of the WPSH may be inappropriate due to global warming, which has produced artificial trends in the lifted isobaric surface at middle and lower latitudes. Huang et al. (2015) reinvestigated the WPSH interdecadal variation in multiple WPSH-associated low-level variables, such as the eddy geopotential height, horizontal winds and relative vorticity. Their results showed that all these variables exhibit consistent signals, suggesting that the WPSH has been recessed eastward during 1979–2009 relative to 1948–1978. They further documented that the Indian summer monsoon played an important role in transporting water vapor into the middle and lower reaches of the Yangtze

River valley associated with the eastward recessed WPSH during 1979–2009, possibly contributing to the excessive rainfall over the middle and lower reaches of the Yangtze River valley since the late 1970s.

Due to the significant effects of the WPSH, assessing and projecting the WPSH in climate models are important issues, which have been intensively studied for decades. Recently, climate models from the Coupled Model Intercomparison Project Phase 5 (CMIP5), with generally higher resolution and a broader set of experiments compared with CMIP3, have been coordinated for use in the Intergovernmental Panel on Climate Change Fifth Assessment Reports (IPCC AR5) (Taylor et al. 2012). Many researchers have investigated the performances of the CMIP5 models in terms of the Asian summer monsoon (Jiang and Tian 2012; Sperber et al. 2012), regional and global precipitation (Chen and Sun 2013; Chen et al. 2014; Gao et al. 2015), decadal variation of the linkage between the East Asian winter monsoon and the El Niño-Southern Oscillation (Wang et al. 2013b), climate extremes in China (Chen and Sun 2015) and certain other atmospheric and oceanic processes. In terms of the WPSH, the previous evaluation and projection focused mainly on the geopotential height field at 500 hPa (e.g., Huang et al. 2013a, b; Xin et al. 2013; Liu et al. 2014), which could be affected by the artificial trend caused by global warming, as previously mentioned, especially when evaluating decadal variations of the WPSH and projecting WPSH variation in the future. Therefore, re-evaluation and re-projection for the WPSH are necessary after removing the aforementioned artificial influence.

This paper is organized as follows. The data, model and method are introduced in Sect. 2. Section 3 evaluates the performance of the CMIP5 models in capturing the mean state of the WPSH based on the fields of the eddy geopotential height and horizontal winds. The models' abilities to reproduce the interannual and interdecadal variations of the WPSH are analyzed in Sect. 4. Section 5 discusses the projection of the WPSH in the future. Finally, a summary is provided in Sect. 6.

2 Data and method

The WPSH appears to be much more stable and stronger in the lower troposphere than in the middle troposphere, and its low-level western and northwestern edges feature southerlies or southwesterlies that transport amount of water vapor, influencing significantly the East Asian summer climate (Lu 2002; Lu et al. 2008). Therefore, we predominantly analyze the WPSH at 850 hPa in this study. The historical simulations of 28 CMIP5 models for the period of 1950–2005 are evaluated. Table 1 lists the basic

Table 1 Description of the 28 CMIP5 models used in this study

Model name	Institute/country	AGCM resolution (ion × lat)
ACCESS1-0	CAWCR/Australia	1.875° × 1.26°
ACCESS1-3	CAWCR/Australia	1.875° × 1.26°
bcc-csm1-1	BCC/China	2.8° × 2.8°
CanESM2	CCCMA/Canada	2.8° × 2.8°
CCSM4	NCAR/USA	1.25° × 0.94°
CESMI-BGC	NSF-DOE-NCAR/USA	2.5° × 1.9°
CESMI-CAM5	NSF-DOE-NCAR/USA	1.25° × 0.94°
CMCC-CESM	CMCC/Italy	3.75° × 3.75°
CMCC-CM	CMCC/Italy	0.75° × 0.75°
CNRM-CM5	CNRM-CERFACS/France	1.4° × 1.4°
FGOALS-g2	LASG-CESS/China	2.8° × 2.8°
GFDL-CM3	NOAA GFDL/USA	2.5° × 2.0°
GFDL-ESM2G	NOAA GFDL/USA	2.5° × 2.0°
GISS-E2-H	NASA GISS/USA	2.5° × 2.0°
GISS-E2-R	NASA GISS/USA	2.5° × 2.0°
HadCM3	MOHC/UK	3.75° × 2.5°
inmcm4	INM/Russia	2.0° × 1.5°
IPSL-CM5A-LR	IPSL/France	3.75° × 1.875°
IPSL-CM5A-MR	IPSL/France	2.5° × 1.25°
IPSL-CM5B-LR	IPSL/France	3.75° × 1.875°
MIROC5	MIROC/Japan	1.4° × 1.4°
MIROC-ESM	MIROC/Japan	2.8° × 2.8°
MPI-ESM-LR	MPI-M/Germany	1.9° × 1.9°
MPI-ESM-MR	MPI-M/Germany	1.875° × 1.875°
MPI-ESM-P	MPI-M/Germany	1.9° × 1.9°
MRI-CGCM3	MRI/Japan	1.1° × 1.1°
NorESM1-M	NCC/Norway	2.5° × 1.875°
NorESM1-ME	NCC/Norway	2.5° × 1.875°

information for these 28 CMIP5 models, including the horizontal resolution of the atmospheric component. The projection simulations for the period of 2006–2100 under the representative concentration pathway leading to a radiative forcing level of 8.5 W/m^2 by 2100 (RCP8.5) (van Vuuren et al. 2011) are used to project the future variations in the WPSH. All the model datasets are interpolated into a common horizontal resolution of 2.5° × 2.5° via a bilinear or area-based interpolation algorithm. Additionally, the monthly mean data in the National Centers for Environmental Prediction/National Center for Atmospheric Research (NCEP/NCAR) reanalysis 1 (Kalnay et al. 1996) with a horizontal resolution of 2.5° is used as verification data. Our analysis focuses solely on the summer months of June–August (JJA).

A Taylor diagram with three statistical measures of the spatial correlation coefficient (SCC), the root mean square error (RMSE) and the standard deviation ratio (SDR) is used to quantify model fidelity for the mean state of the WPSH (Taylor 2001). Following Huang et al. (2015), we use the simple difference between means for the periods 1979–2005 and 1950–1978 to characterize the interdecadal variation of the WPSH. The statistical significance is assessed using the Student's *t* test.

3 Simulation of the climatology of the WPSH

To avoid the artificial influences caused by global warming, we first examine the features of the eddy geopotential height (H′) field at 850 hPa (hereafter H′850), in which H′ = H− H̄, where H is the geopotential height and H̄ is the zonal mean of H. Figure 1 shows the climatology of the observed and simulated summer H′850. The WPSH indicated by the positive eddy geopotential height is a dominant high-pressure system over Pacific, accompanied by a negative eddy geopotential height over East Asia, which represents the Asian low system (Fig. 1a). The CMIP5 models generally reproduce the positive H′850 over Asia and the negative H′850 over the Pacific, although biases exist in intensity and position (Fig. 1b1–r2). Figure 2 shows the position of the western edge of the WPSH (the contour line of 0 gpm over the western Pacific) in the CMIP5 model simulations and NCEP. Compared with the position of the western edge of the WPSH in the NCEP, i.e., near 140°E and 20°N, a more westward-extended WPSH appears in the FGOALS-g2, MIROC5 and the MIROC-ESM models and a somewhat eastward- or northward-recessed WPSH is produced by bcc-csm1-1, CanESM2, GFDL-CM3, inmcm4, and MPI models. Additionally, a dramatic underestimation of the WPSH is found in three IPSL models and the MRI-CGCM3 model, with the positive eddy geopotential height only appearing east of 170°E over the Pacific. The other CMIP5 models, such as ACCESS1, CNRM–CM5, HadCM3 and NorESM1 models, perform generally well in capturing the intensity and the position of the climatological H′850 over Pacific, which is indicative of a reasonable ability reproducing the mean state of the WPSH (Figs. 1, 2). Similarly, the CMIP5 models' abilities to capture the climatological WPSH can also be observed in the climatology maps of the summer 850-hPa geopotential height and horizontal winds (figures not shown). Moreover, it should be noticed that most of the CMIP5 models fail to capture the mean state of the WPSH described in the climatology map of the 500-hPa geopotential height due to larger systematic errors (Liu et al. 2014). Therefore, compared with the 500-hPa geopotential height, the use of the 850-hPa eddy geopotential height field in the CMIP5 models to project the future variations of the WPSH seems to be more creditable.
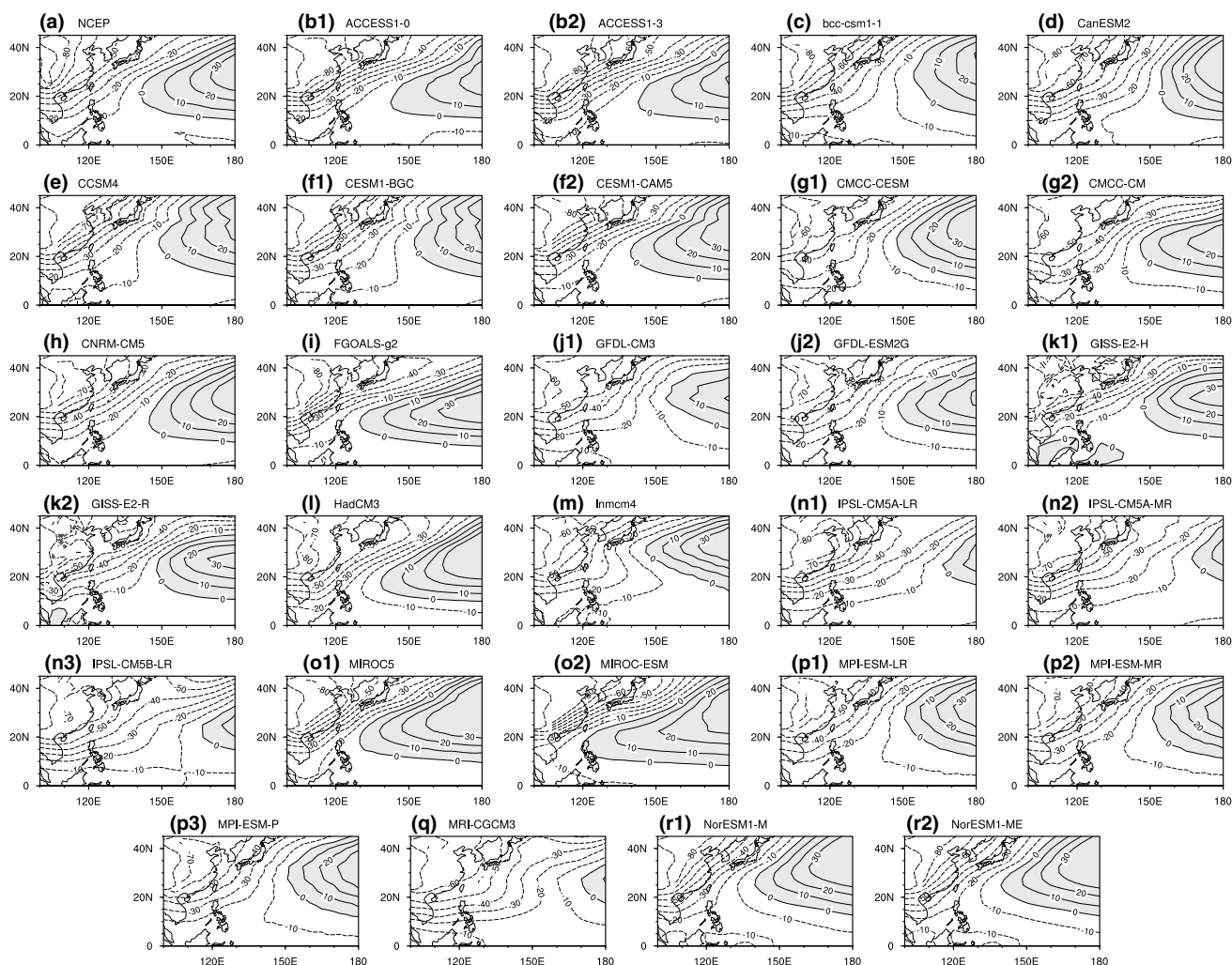
Fig. 1 The climatology of the JJA-mean eddy geopotential height at 850 hPa (H′850) (gpm) during 1950–2005 from the NCEP/NCAR reanalysis data (**a**) and CMIP5 model simulations (**b1–r2**). The *shaded regions* denote H′850 values >0 gpm, and the *thick dashed lines* indicate the topographic contour of 1500 m

More quantitative measurements can be obtained from a Taylor diagram (Fig. 3). Specifically, the azimuthal angle represents the spatial correlation coefficient (SCC), the distance apart between the model code and REF (reference, namely observation) indicates the root mean square error (RMSE) and the radial distance from the origin is the standard deviation ratio (SDR) between a simulation and an observation. The SCC and RMSE measure the model quality with respect to the variable's spatial distribution, whereas the SDR reflects the model quality with respect to the variable's amplitude or spatial variability. Smaller distances between the model code and the REF in the Taylor diagram indicate better performances for the corresponding model. For the climatological summer H′850 over the western Pacific (0°–145°N, 110°–180°E) (Fig. 3a), the SCCs in all 28 CMIP5 models are above 0.80, and half are above 0.95, which are statistically significant at the 99.9 % confidence level (0.14). The RMSEs are generally <0.65 gpm, except the IPSL-CM5B-LR and MRI-CGCM3 models, which have slightly larger values of 0.79 and 0.75 gpm, respectively. These results represent the CMIP5 models' capacity in reproducing the geographical distribution of H′850 over the western Pacific. Meanwhile, the CMIP5 models with SDRs between 0.75 and 1.28 also well capture the spatial variability of the climatological H′850. Most CMIP5 models, with SCCs of 0.73–0.98, RMSEs of 0.38–0.76 and SDRs of 0.78–1.32, reasonably reproduce the main features of the spatial distribution and amplitude of the climatological summer zonal wind at 850 hPa over the western Pacific (Fig. 3b). One significant outlier is the MIROC-ESM model with an SDR of 1.62 and a relatively high RMSE value of 1.12. Overall, according to Fig. 3, most CMIP5 models reliably reproduced the spatial distribution and variability of the WPSH.
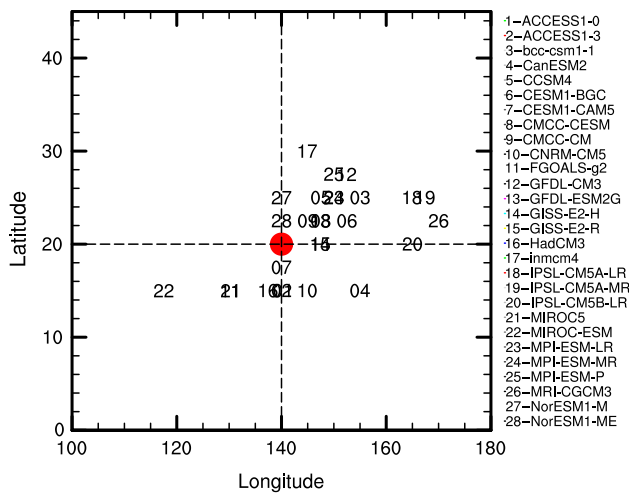
Fig. 2 The westernmost location of the contour line of 0 gpm in the climatological JJA 850-hPa eddy geopotential height over the western Pacific in the CMIP5 models and NCEP (*red dot*)

4 Performance with respect to the interdecadal variations of the WPSH

Following Huang et al. (2015), we defined the WPSH index (WPSHI) as the regionally averaged summer $H'850$ over the maximum interannual variability center (15°–30°N, 120°–150°E) of the western edge of the WPSH to characterize the variability of the WPSH. Figure 4 shows the linear trend of the normalized summer WPSHI from 1950 to 2005 for the NCEP data and CMIP5 model simulations. The NCEP WPSHI displays a significant decreasing trend of −0.027 (significant at the 99.9 % confidence level)

during 1950–2005, indicating a weakened and eastward-recessed WPSH in the late 1970s (Fig. 4). As shown in Fig. 4, 11 CMIP5 models generally capture this decreasing trend. In particular, the trends of the simulated WPSHIs in the models bcc-csm1-1, CESM1-CAM5, GFDL-ESM2G, inmcm4, and MPI-ESM-Pare −0.018, −0.011, −0.014, −0.011, and −0.015, which are significant at the 97, 80, 90, 83, and 92 % confidence levels, respectively. However, the rest of CMIP5 models fail to capture this decreasing trend, with no interdecadal variation in 8 models and even opposite increasing trends in 9 models (Fig. 4). For example, the ACCESS1-0, GISS-E2-H, and IPSL-CM5A-LR models exhibit no trends in the WPSHIs, and the MIROC5 and MRI-CGCM3 models exhibit significant increasing trends of 0.026 and 0.019, respectively.

The interdecadal signals of the WPSH can be further observed in the difference map of the 850-hPa winds between 1979–2005 and 1950–1978. A significant anomalous cyclone appears over the western Pacific, suggesting a weakened WPSH during 1979–2005 relative to 1950–1978 (Fig. 5a). Meanwhile, the anomalous northeasterly winds prevail from North to South China in observation, indicating a weakened EASM in 1979–2005 compared to 1950–1978 (Wang 2001) (Fig. 5a). The anomalous cyclone over the western Pacific is generally reproduced by 9 CMIP5 models, but with the biases in position and intensity relative to the observation. In particular, the bcc-csm1-1, CESM1-CAM5, GFDL-ESM2G and inmcm4 models exhibit the best performances, with the significant anomalous cyclone appearing over the western Pacific. The ACCESS1-0, CanESM2, CESM1-BGC, GFDL-CM3 and NorESM1-ME models also capture the anomalous cyclone
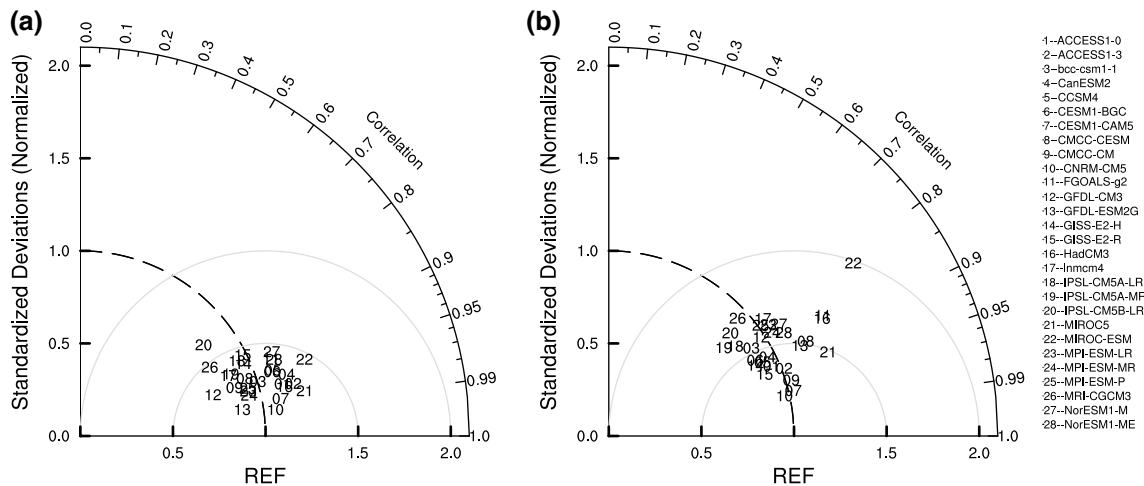

Fig. 3 Taylor diagram of simulated climatological JJA eddy geopotential height (**a**) and zonal wind (**b**) at 850 hPa during 1950–2005 over the western Pacific (0°–45°N, 110°–180°E) with respective to observation (namely Reference, REF). The radial distance of the model code from the origin is the standard deviation ratio of the

model relative to the observation. The spatial correlation coefficient between the model simulation and the observation is expressed as the azimuthal position of the model code. The root-mean-square error is given by the distance between themodel code and the REF
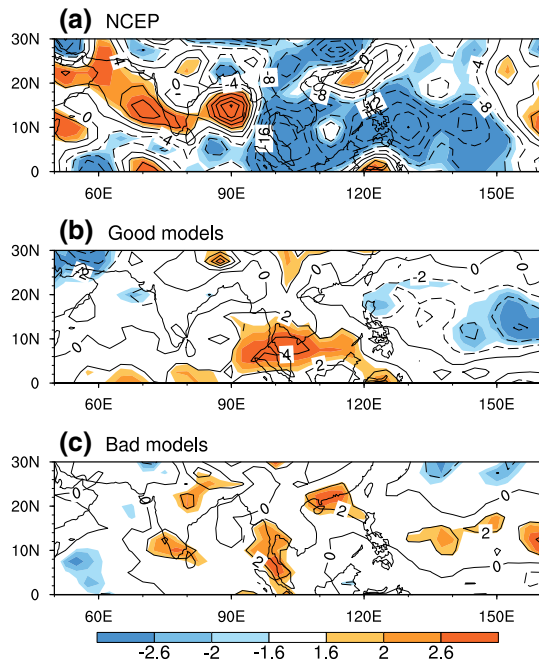
Fig. 4 The linear trend of the normalized JJA WPSH index (WPSHI) (%) during 1950–2005 in the NCEP and the CMIP5 model simulations

over the western Pacific, but the intensities of the simulated cyclonic anomalies are weaker than the observation and are not statistically significant. Interestingly, the 9 models that

produce an anomalous cyclone over the western Pacific are the same models that capture the decreasing trend of the WPSH index. The four best models is the models with most significant decreasing trends (Fig. 4). However, the remaining 19 CMIP5 models perform very poorly in representing this anomalous cyclone, with no interdecadal signals or even significant anomalous anticyclone over the western Pacific (e.g., the MIROC5 model).

The cause of the differences in the ability to simulate the interdecadal WPSH variations between the 9 good models and the other 19 bad models is further analyzed. It has been confirmed that the Indian Ocean-Western Pacific warming can induce a strong and westward extended WPSH (e.g., Yang et al. 2007; Li et al. 2008; Zhou et al. 2009). All CMIP5 models successfully capture the interdecadal increased SSTs in the late 1970s in the Indian ocean-western Pacific regions (figure not shown). It seems to imply that all CMIP5 models should consequently produce an

Fig. 5 The difference in the JJA horizontal winds at 850 hPa between 1979–2005 and 1950–1978 for the NCEP (**a**) and the CMIP5 model simulations (**b1–r2**). *Shading* indicates significance at the 95 % confidence level using Student's *t* test

Fig. 6 The difference in JJA 500-hPa vertical p velocity ($\times$ 0.001 Pa s^{-1}) between 1979–2005 and 1950–1978 in the NCEP (**a**), the multi-model ensemble of the 9 good models (**b**) and the multi-model ensemble of the 19 bad models. The contour interval is 4 Pa s^{-1} (2 Pa s^{-1}) in Panel **a** (Panel **b** and **c**). *Dark*, *medium* and *light blue* and *red shading* indicate significance at the 99, 95 and 90 % confidence levels, respectively, using Student's t test. The 9 good models are ACCESS1-0, bcc-csm1-1, CanESM2, CESM1-CAM5, CESM1–BGC, GFDL–CM3, GFDL–ESM2G, inmcm4 and NorESM1-ME

Fig. 7 The 9-year running mean of the JJA the traditional WPSH index based on the 850-hPa geopotential height (**a**) and the WPSHI based on the 850-hPa eddy geopotential height (**b**) from 2006 to 2100 under the RCP8.5 scenario from the projections of the four best CMIP5 models (*thin dash lines*) and the multi-model ensemble (MME) (*thick solid line*). *Shaded areas* represent the MME's uncertainty which is obtained from one standard deviation of individual models departure from MME

westward extended WPSH, however, it is contrary to the above evaluated results. For the SST role in affecting the interdecadal variation of the WPSH, Huang et al. (2015) suggested the different active roles between the North Indian Ocean (NIO) and the western North Pacific (WNP). Particularly, they examined the interdecadal signal in the 500-hPa vertical p velocity. The dominant descent over the NIO suggests a recharging phase of the NIO on the interdecadal scale, and the large ascent area over the WNP indicates the vital role of the WNP in affecting the atmospheric circulations over that region (Fig. 6a). Through local wind-evaporation-SST feedback, the cool western north Pacific favors a westward and enhanced WPSH (Wang et al. 2000, 2013a; Wu et al. 2010). Therefore, they suggested that the recharging phase of the Indian ocean and the western north Pacific warming in the late 1970s may together contribute to the interdecadal weakening of the WPSH. Considering this speculation, we compare the model performances in simulating the interdecadal signal in the 500-hPa vertical p velocity to examine the model ability for capturing the different active role of SST. The multi-model ensemble of the 9 good models generally reproduce the interdecadal signals
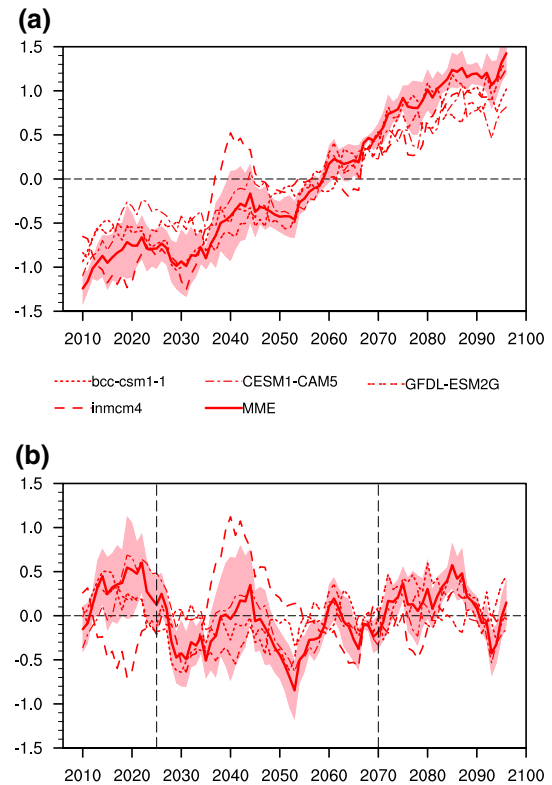
of the 500-hPa vertical p velocity, with descent appearing over the NIO and ascent locating over the WNP, although certain biases exist in position and intensity (Fig. 6b). However, the 19 bad models simulate a consistent descent spanning from the NIO to the WNP, thus failing to reproduce the ascent over the WNP (Fig. 6c). Thus, the ability of the 9 good models to reproduce the interdecadal WPSH variation may be attributed to the ability of these models in capturing the different roles of the NIO and the WNP in affecting atmospheric circulations on the interdecadal scale.

5 Projection of the WPSH under RCP8.5

Based on the above analyses, the four CMIP5 models that were best able to reproduce the interdecadal WPSH variations (including the decreasing trend of the WPSH index and the anomalous cyclone over western Pacific)—bcc-csm1-1, CESM1-CAM5, GFDL-ESM2G and inmcm4— were selected to make future projections for the 21st

In addition to the above-defined WPSHI based on H'850, the traditional WPSH index, similar to the WPSHI but based on the 850-hPa geopotential height, was also analyzed for comparison. Figure 7 shows the 9-year running mean of the normalized traditional WPSH index and WPSHI from 2006 to 2100. Not surprisingly, due to the exacerbated effects of global warming on the increased geopotential height in twentyfirst century, the traditional WPSH indice in four CMIP5 models and in the MME all exhibit significant increasing trends (e.g. the trend in MME is 0.030, significant at 99.9 % confidence level) and predict a gradually strengthening WPSH (Fig. 7a). In fact, based on the projections using the geopotential height field, the strengthened and westward-extended features of the future WPSH have been illustrated by many researchers (e.g., Seo et al. 2013; Xin et al. 2013; Liu et al. 2014). However, after removing the artificial trends caused by global warming, no significant linear trend exists in the WPSHIs. This result is consistent with those of He and Zhou (2015), who documented that the projected changes in the WPSH intensity are approximately zero under both RCP4.5 and RCP8.5 scenarios. In addition, deriving from the inmcm4 model with different projected phase or magnitude, the MME's uncertainty before 2045 is larger than it after 2045 for both traditional WPSH index case and WPSHI case.

According the interdecadal signals in WPSHI, the MME projects the WPSH is in a positive phase during 2010–2025 and 2071–2100 and in a negative phase during 2026–2070. To verify this WPSH future interdecadal variation, we examined the differences in the 850-hPa horizontal winds between the positive phase periods (2010–2025 and 2071–2100) and the negative phase period (2026–2070) in the MME (Fig. 8). In Fig. 8a, significant anticyclonic anomalies appear over the western Pacific. For each positive phase period, the significant anticyclone anomalous can also been seen in the difference maps (Fig. 8b, c). In the difference maps for the relative vorticity at middle-lower levels (1000–500 hPa) along $15°–30°N$, the remarkable significant negative anomalies of the relative vorticity span the western Pacific region (Fig. 9). Based on a stronger WPSH corresponding to stronger anticyclonic circulation and higher negative vorticity over the western Pacific, the significant anticyclonic anomalies in the 850-hPa winds and the negative anomalies in the relative vorticity suggest that the WPSH may not gradually strengthen in the twentyfirst century (as projected by the traditional WPSH index) and may instead to weaken during 2026–2070 relative to 2010–2025 and 2071–2100. These consistent interdecadal WPSH
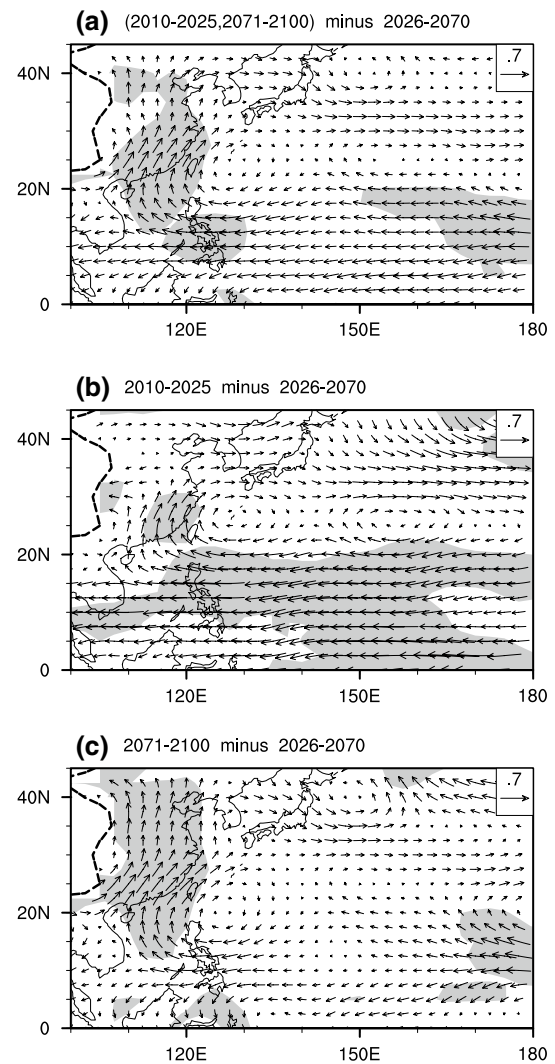

Fig. 8 Differences in the horizontal winds at 850 hPa in the four best CMIP5 models' ensemble between the WPSH positive periods (2010–2025 and 2071–2100) and the negative period (2026–2070) (**a**). Panels **b** and **c** are same as in panel **a** but for the positive period of 2010–2025 in panel **b**, and 2071–2100 in panel **c**. *Shading indicates* significance at the 95 % confidence level using Student's *t* test

variations in the future 850-hPa winds and relative vorticity imply that the projections based on the WPSHI are reliable. Therefore, compared the traditional WPSH index based on geopotential height, which can be affected by the artificial trends caused by global warming, the WPSHI based on the eddy geopotential height is better suited to project future WPSH variations.

6 Summary and discussion

The western Pacific subtropical high is a dominant anticyclonic circulation over the subtropical Pacific and exerts
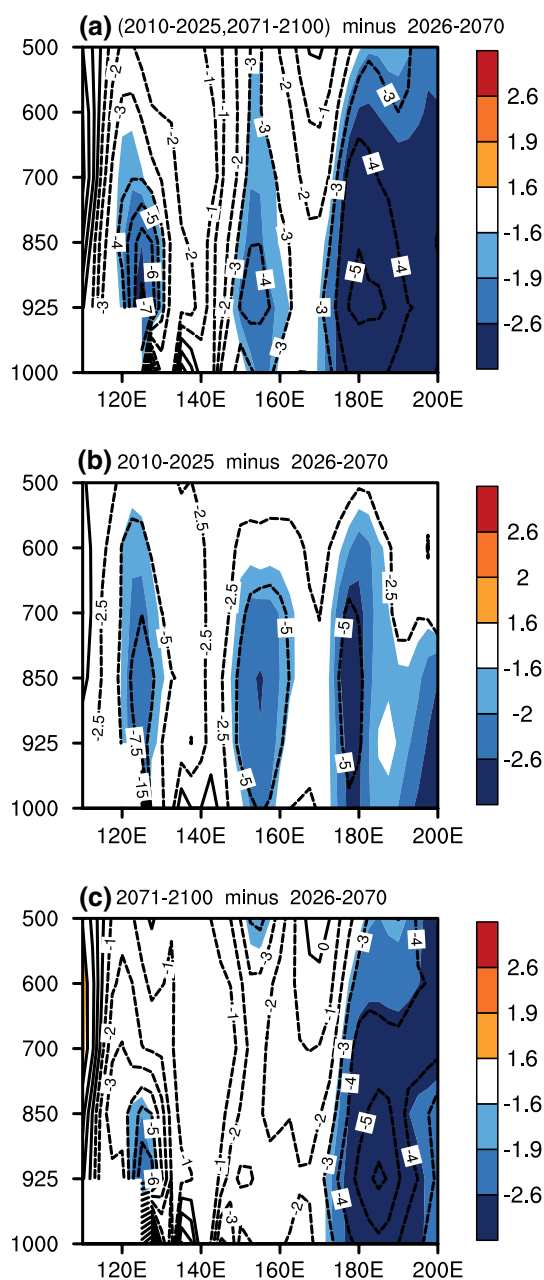
Fig. 9 Same as in Fig. 8, but for the difference in the cross-section of the JJA relative vorticity along 15°–30°N at the middle and lower levels (1000–500 hPa). *Dark, medium and light blue* and *red shading* indicate significance at the 99, 95, and 90 % confidence levels, respectively, using Student's *t* test

large influences on the East Asian summer climate, especially the low-level WPSH with southerlies or southwesterlies along its lower-level western or southern edges. This study assesses the ability of 28 CMIP5 models to simulate the summer low-level WPSH during 1950–2005. We primarily investigated the fields of eddy geopotential height and horizontal winds at 850 hPa to avoid the artificial influences caused by global warming. The results show that

most of the models generally performed well in reproducing the spatial distribution and amplitude of the WPSH, excluding three IPSL models with significant underestimations and the MIROC5 model with a significant overestimation. Four models (bcc-csm1-1, CESM1-CAM5, GFDL-ESM2G and inmcm4) successfully captured the significant cyclonic anomalies in the 850-hPa winds over the western Pacific during 1979–2005 relative to 1950–1978 and the significant decreasing trend in the WPSH index (WPSHI) during 1950–2005. Therefore, these models generally captured the eastward recession of the WPSH in the late of 1970s, which may be attributed to the models' ability to reproduce the recharging phase of the North Indian Ocean and the vital role of the western North Pacific in affecting the atmospheric circulations on the interdecadal scale.

The four models that performed best in reproducing the historical interdecadal WPSH variation were selected to project the WPSH variation into the future of the twentyfirst century under RCP8.5. Using the WPSHI based on eddy geopotential height, the WPSH is projected to be weaker during 2026–2070 relative to 2010–2025 and 2071–2100. These future WPSH interdecadal variations are further verified by the significant anticyclonic anomalies in the 850-hPa winds and the significant negative anomalies in the relative vorticity at middle-lower levels (1000–500 hPa) along 15°–30°N over the western Pacific in the difference maps between the positive phase periods (2010–2025 and 2071–2100) and the negative phase period (2026–2070). Considering the isobaric surface at the middle-lower latitudes could be further lifted in global future further warming, the artificial trends in the increased geopotential height would be exacerbated, thus the traditional WPSH index based upon geopotential height may not be suitable for projecting future WPSH changes.

The possible reason for the weakened WPSH during 2025–2070 is now discussed. Using the diagnostic study and numerical simulation, He and Zhou (2014) suggested that the SST gradient between the tropical Indian Ocean and the tropical western Pacific dominates the projected WPSH intensity under both the RCP4.5 and RCP 8.5 scenarios. A stronger (weaker) warming in the tropical Indian Ocean—TIO, 10°S–10°N, 50°E–100°E—stimulates warm (cold) Kelvin waves, which increase (decrease) the WPSH intensity via wave-induced Ekman divergence (convergence). A weaker (stronger) warming in the tropical western Pacific—TWP, 10°S–10°N, 150°E–180°E—increases (decreases) the WPSH intensity via an anticyclonic (cyclonic) Rossby wave response to the northwest. Therefore, we examine the future changes of the differences in the normalized regionally averaged SST between the TIO and the TWP (i.e., the TIO-TWP zonal SST gradient) during 2006–2100 (Fig. 10). The correlation coefficient between the 9-year running mean WPSHI and TIO-TWP SST zonal gradient is 0.50 during 2006–2100 in the MME,
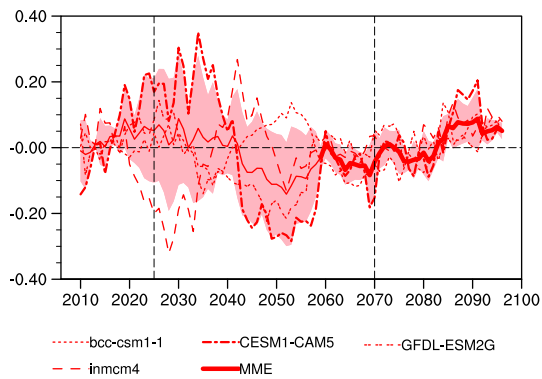
Fig. 10 Same as in Fig. 7, but for the TIO-TWP SST zonal gradient, which is defined as the difference in the normalized regionally averaged SST between the TIO (10°S–10°N, 50°E–100°E) and the TWP (10°S–10°N, 150°E–180°E)

exceeding the 99.9 % confidence level. Based on this significant positive correlation, the general negative phase of the TIO-TWP zonal SST gradient during 2025-2070 may give a clue for the weakened WPSH (Fig. 10). However, the primarily negative phase of the TIO-TWP zonal SST gradient is not completely consistent with the negative phase of the WPSH. This disagreement means that there may still be other factors responsible for the weakened WPSH during 2025-2070. Therefore, further analysis based on more quantitative diagnose, as well as state-of-the art climate models, is needed in the future work.

References

Chang CP, Zhang Y, Li T (2000) Interannual and interdecadal variations of the East Asian summer monsoon and tropical Pacific SSTs. Part I: roles of the subtropical ridge. J Clim 13:4310–4325

Chen H, Sun J (2013) Projected change in East Asian summer monsoon precipitation under RCP scenario. Meteorol Atmos Phys 121:55–77. doi:10.1007/s00703-013-0257-5

Chen H, Sun J (2015) Assessing model performance of climate extremes in China: an intercomparison between CMIP5 and CMIP3. Clim Change: 1–15%@ 0165–0009

Chen Y, Zhang H, Zhou R, Wu H (2001) Relationship between the ground surface temperature in Asia and the intensity and location of subtropical high in the western Pacific (in Chinese). Chin J Atmos Sci 25:515–522

Chen H, Sun J, Chen X (2014) Projection and uncertainty analysis of global precipitation-related extremes using CMIP5 models. Int J Climatol 34:2730–2748. doi:10.1002/joc.3871

Chia HH, Ropelewski CF (2002) The interannual variability in the genesis location of tropical cyclones in the northwest Pacific. J Clim 15:2934–2944

Ding YH (1994) The summer monsoon in East Asia.Monsoons over China. Kluwer, Dordrecht, pp 1–9

Gao Y, Wang H, Jiang D (2015) An intercomparison of CMIP5 and CMIP3 models for interannual variability of summer precipitation in Pan-Asian monsoon region. Int J Climatol. doi:10.1002/joc.4245

Gong D-y, He X-z (2002) Interdecadal change in western Pacific subtropical high and climatic effects (in Chinese). Acta Geogr Sin 57:185–193

Gong DY, Ho CH (2002) Shift in the summer rainfall over the Yangtze River valley in the late 1970s. Geophys Res Lett. doi:10.1029/2001gl014523

He C, Zhou T (2015) Responses of the Western North Pacific Subtropical High to Global Warming under RCP4.5 and RCP8.5 Scenarios Projected by 33 CMIP5 Models: the dominance of tropical Indian Ocean–tropical western Pacific SST gradient. J Clim 28:365–380

He C, Zhou T, Zou L, Zhang L (2012) Two interannual variability modes of the Northwestern Pacific Subtropical Anticyclone in boreal summer. Sci Chin Earth Sci. doi:10.1007/s11430-012-4443-y

Ho C-H, Baik J-J, Kim J-H, Gong D-Y, Sui C-H (2004) Interdecadal changes in summertime typhoon tracks. J Clim 17:1767–1776

Hoskins BJ (1996) On the existence and strength of the summer subtropical anticyclones. Bull Am Meteorol Soc 77:1287–1292

Hu ZZ (1997) Interdecadal variability of summer climate over East Asia and its association with 500 hPa height and global sea surface temperature. J Geophys Res. doi:10.1029/97jd01052

Huang S (1963) A study of the longitudinal movement and forecasting of subtropical anticyclones (in Chinese). Acta Meteor Sin 33:320–332

Huang Y, Li X (2015) The interdecadal variation of the western Pacific subtropical high as measured by 500 hPa eddy geopotential height. Atmos Oceanic Sci Lett. doi:10.3878/AOSL20150038

Huang R, Sun F (1994) Impacts of the thermal state and the convective activities in the tropical western warm pool on the summer climate anomalies in East Asia (in Chinese). Chin J Atmos Sci 18:141–151

Huang R, Wu Y (1989) The influence of ENSO on the summer climate change in China and its mechanism. Adv Atmos Sci 6:21–32

Huang SS, Yu ZH (1962) On the structure of the subtropical highs and some associated aspects of the general circulation of atmosphere (in Chinese). Acta Meteor Sin 31:339–359

Huang G, Hu K, Xie S-P (2010) Strengthening of Tropical Indian Ocean Teleconnection to the Northwest Pacific since the Mid-1970s: an atmospheric GCM study*. J Clim 23:5294–5304

Huang DQ, Zhu J, Zhang YC, Huang AN (2013a) Uncertainties on the simulated summer precipitation over Eastern China from the CMIP5 models. J Geophys Res Atmos 118:9035–9047

Huang Y, Wang H, Zhao P (2013b) Is the interannual variability of the summer Asian–Pacific oscillation predictable? J Clim 26:3865–3876

Huang Y, Wang H, Fan K, Gao Y (2015) The western Pacific subtropical high after the 1970s: westward or eastward shift? Clim Dyn 44:2035–2047

Jiang D, Tian Z (2012) East Asian monsoon change for the 21st century: results of CMIP3 and CMIP5 models. Chin Sci Bull 58:1427–1435

Kalnay E et al (1996) The NCEP/NCAR 40-year reanalysis project. Bull Am Meteorol Soc 77:437–471

Kuang XY, Zhang YC (2006) Impact of the position abnormalities of East Asian subtropical westerly jet on summer precipitation in middle-lower reaches of Yangtze River (in Chinese). Plateau Meteorol 25:382–389

Lau KM, Li MT (1984) The monsoon over East Asia and its global association—a survey. Bull Am Meteor Soc 65:116–125

Li CY, Wang JT, Lin SZ, Cho HR (2004) The relationship between East Asian summer monsoon activity and northward jump of the upper westerly jet location (in Chinese). Chin J Atmos Sci 28:641–658

Li S, Lu J, Huang G, Hu K (2008) Tropical Indian Ocean Basin warming and East Asian summer monsoon: a multiple AGCM study. J Clim 21:6080–6088

Liao QS, Zhao ZG (1990) The impacts of the East Asian blocking situation on the rainfall over China and its relationship with the western Pacific subtropical high Essays on the Long-term Weather Forecast. China Metorological Press, Beijing, pp 125–134 **(in Chinese)**

Liu Y, Li W, Zuo J, Hu Z (2014) Simulation and projection of the western Pacific subtropical high in CMIP5 Models. J Meteorol Res 28:327–340

Lu R (2002) Indices of the summertime western North Pacific subtropical high. Adv Atmos Sci 19:1004–1028

Lu R, Dong B (2001) Westward extension of North Pacific subtropical high in summer. J Meteorol Soc Jpn 79:1229–1241

Lu R, Li Y, Ryu CS (2008) Relationship between the zonal displacement of the western Pacific subtropical high and the dominant modes of low-tropospheric circulation in summer. Prog Nat Sci 18:161–165

Miyasaka T, Nakamura H (2005) Structure and formation mechanisms of the northern hemisphere summertime subtropical highs. J Clim 18:5046–5065

Nitta T, Hu ZZ (1996) Summer climate variability in China and its association with. J Meteorol Soc Jpn 74:425–445

Rodwell MJ, Hoskins BJ (2001) Subtropical anticyclones and summer monsoons. J Clim 14:3192–3211

Seager R, Murtugudde R, Naik N, Clement A, Gordon N, Miller J (2003) Air–sea interaction and the seasonal cycle of the subtropical anticyclones. J Clim 16:1948–1966

Seo KH, Ok J, Son JH, Cha DH (2013) Assessing future changes in the east Asian summer monsoon using CMIP5 coupled models. J Clim 26:7662–7675

Sperber KR et al (2012) The Asian summer monsoon: an intercomparison of CMIP5 vs. CMIP3 simulations of the late 20th century. Clim Dyn 41:2711–2744

Sui CH, Chung PH, Li T (2007) Interannual and interdecadal variability of the summertime western North Pacific subtropical high. Geophys Res Lett. doi:10.1029/2006GL029204

Sun S, Ying M (1999) Subtropical high anomalies over the western Pacific and its relations to the Asian monsoon and SST anomaly. Adv Atmos Sci 16:559–568

Tao SY (1963) On the summer synoptic systems in the subtropics over China (in Chinese). Science Press, Beijing

Tao SY, Chen LX (1987) A review of recent research on the East Asian summer monsoon in China Monsoon Meteorol, vol 7. Oxford University Press, pp. 60-92

Tao SY, Xu SY (1962) Circulation characteristics in assimilation with president summer drought and flood in the Yangtze-Huaihe River reaches. Acta Meteor Sin 32:1–18

Tao SY, Zhu FK (1964) The 100 mb flow patterns in southern Asia in summer and its relation to the advance and retreat of the west2 pacific subtropical anticyclone over the far east (in Chinese). Acta Meteorol Sin 34:385–396

Taylor KE (2001) Summarizing multiple aspects of model performance in a single diagram. J Geophys Res Atmos 106:7183–7192

Taylor KE, Stouffer RJ, Meehl GA (2012) An Overview of CMIP5 and the experiment design. Bull Am Meteorol Soc 93:485–498

Ting M (1994) Maintenance of northern summer stationary waves in a GCM. J Atmos Sci 51:3286–3308

van Vuuren DP et al (2011) The representative concentration pathways: an overview. Clim Change 109:5–31

Wang HJ (2001) The weakening of the Asian monsoon circulation after the End of 1970's. Adv Atmos Sci 18:376–386

Wang H, Chen H (2012) Climate control for southeastern China moisture and precipitation: Indian or East Asian monsoon? J Geophys Res Atmos. doi:10.1029/2012JD017734

Wang B, Wu R, Fu X (2000) Pacific–East Asian teleconnection: How does ENSO affect east Asian climate? J Clim 13:1517–1536

Wang B, Wu R, Lau KM (2001) Interannual variability of the Asian summer monsoon: contrasts between the Indian and the western North Pacific–East Asian Monsoons*. J Clim 14:4073–4090

Wang B, Xiang B, Lee J-Y (2013a) Subtropical High predictability establishes a promising way for monsoon and tropical storm predictions. Proc Natl Acad Sci 110:2718–2722

Wang H, He S, Liu J (2013b) Present and future relationship between the East Asian winter monsoon and ENSO: results of CMIP5. J Geophys Res Oceans. doi:10.1002/jgrc.20332

Wu GX, Liu YM (2003) Summertime quadruplet heating pattern in the subtropics and the associated atmospheric circulation. Geophys Res Lett. doi:10.1029/2002GL016209

Wu B, Li T, Zhou T (2010) Relative contributions of the Indian Ocean and local SST anomalies to the maintenance of the western north Pacific anomalous anticyclone during the El Niño Decaying Summer*. J Clim 23:2974–2986

Xin X, Zhang L, Zhang J, Wu T, Fang Y (2013) Climate change projections over east Asia with BCC_CSM1.1 climate model under RCP scenarios. J Meteorol Soc Jpn 91:413–429

Yang H, Sun SQ (2003) Longitudinal displacement of the subtropical high in the western Pacific in summer and its influence. Adv Atmos Sci 20:921–933

Yang J, Liu Q, Xie SP, Liu Z, Wu L (2007) Impact of the Indian Ocean SST basin mode on the Asian summer monsoon. Geophys Res Lett. doi:10.1029/2006GL028571

Ye DZ, Gao YX (1979) Meteorology over Tibetan Plateau. Science Press, Beijing **p278**

Ye DZ, Wu GX (1998) The role of the heat source of the Tibetan Plateau in the general circulation. Meteorol Atmos Phys 67:181–198

Zhang Q, Tao S (2003) The anomalous subtropical anticyclone in western Pacific and their association with circulation over East Asia during summer (in Chinese). Chin J Atmos Sci 27:369–380

Zhang Q, Wu G (2001) The large area flood and drought over Yangtze River valley and its relation to the South Asia High (in Chinese). Acta Meteorol Sin 59:569–577

Zhao B, Yao X, Wu G (2005) The structure and activity characteristics of the western Pacific subtropical anticyclone and its dynamical mechanism during the Meiyu period over the Huaihe River basin in 2003 (in Chinese). Chin J Atmos Sci 29:771–779

Zhou B, Cui X (2008) Hadley circulation signal in the tropical cyclone frequency over the western North Pacific. J Geophys Res Atmos. doi:10.1029/2007JD009156

Zhou T et al (2009) Why the western Pacific subtropical high has extended westward since the late 1970s. J Clim 22:2199–2215

Zhu QG, Lin JR, Shou SW, Tang DS (2000) Theory and Methods of Synoptic Meteorology, 3rd edn. China Metorological Press, Beijing, pp 474–478 **(in Chinese)**

Zhu YL, Wang HJ, Zhou W, Ma JH (2010) Recent changes in the summer precipitation pattern in East China and the background circulation. Clim Dyn 36:1463–1473. doi:10.1007/s00382-010-0852-9